Statistical Hadronization Model analysis of hadron yields in p+Nb and Ar+KCl at SIS18 energies

Agakishiev, G.; Arnold, O.; Balanda, A.; Belver, D.; Belyaev, A.; Berger-Chen, J. C.; Blanco, A.; Böhmer, M.; Boyard, J. L.; Cabanelas, P.; Castro, E.; Chernenko, S.; Destefanis, M.; Dohrmann, F.; Dybczak, A.; Epple, E.; Fabbietti, L.; Fateev, O.; Finocchiaro, P.; Fonte, P.; Friese, J.; Fröhlich, I.; Galatyuk, T.; Garzon, J. A.; Gernhäuser, R.; Gilardi, C.; Göbel, K.; Golubeva, M.; Gonzalez-Diaz, D.; Guber, F.; Gumberidze, M.; Heinz, T.; Hennino, T.; Holzmann, R.; Ierusalimov, A.; Iori, I.; Ivashkin, A.; Jurkovic, M.; Kämpfer, B.; Karavicheva, T.; Koenig, I.; Koenig, W.; Kolb, B. W.; Kornakov, G.; Kotte, R.; Krasa, A.; Krizek, F.; Krücken, R.; Kuc, H.; Kühn, W.; Kugler, A.; Kurepin, A.; Ladygin, V.; Lalik, R.; Lange, J. S.; Lang, S.; Lapidus, K.; Lebedev, A.; Liu, T.; Lopes, L.; Lorenz, M.; Maier, L.; Mangiarotti, A.; Markert, J.; Metag, V.; Michalska, B.; Mihaylov, D.; Michel, J.; Moriniere, E.; Mousa, J.; Müntz, C.; Münzer, R.; Naumann, L.; Pachmayer, Y. C.; Palka, M.; Parpottas, Y.; Pechenov, V.; Pechenova, O.; Pietraszko, J.; Przygoda, W.; Ramstein, B.; Rehnisch, L.; Reshetin, A.; Rustamov, A.; Sadovsky, A.; Salabura, P.; Scheib, T.; Schmah, A.; Schuldes, H.; Schwab, E.; Siebenson, J.; Sobolev, Y. G.; Spataro, S.; Spruck, B.; Ströbele, H.; Stroth, J.; Sturm, C.; Tarantola, A.; Teilab, K.; Tlusty, P.; Traxler, M.; Trebacz, R.; Tsertos, H.; Vasiliev, T.; Wagner, V.; Weber, M.; Wendisch, C.; Wirth, J.; Wisniowski, M.; Wüstenfeld, J.; Yurevich, S.; Zanevsky, Y.;

Originally published:

June 2016

European Physical Journal A 52(2016), 178

DOI: https://doi.org/10.1140/epja/i2016-16178-x

Statistical Hadronization Model analysis of hadron yields in p+Nb and Ar+KCl at SIS18 energies

G. Agakishiev[7],O. Arnold[10,9], A. Balanda[3], D. Belver[18], A. Belyaev[7], J.C. Berger-Chen[10,9], A. Blanco[2], M. Böhmer[10], J. L. Boyard[16], P. Cabanelas[18],E. Castro[18], S. Chernenko[7], M. Destefanis[11],F. Dohrmann[6], A. Dybczak[3], E. Epple[10,9], L. Fabbietti[10,9], O. Fateev[7], P. Finocchiaro[1], P. Fonte[2,b], J. Friese[10], I. Fröhlich[8], T. Galatyuk[5,c], J. A. Garzón[18], R. Gernhäuser[10],C. Gilardi[11], K. Göbel[8], M. Golubeva[13], D. González-Díaz[5], F. Guber[13], M. Gumberidze[5,c], T. Heinz[4], T. Hennino[16], R. Holzmann[4], A. Ierusalimov[7], I. Iori[12,e], A. Ivashkin[13], M. Jurkovic[10], B. Kämpfer[6,d], T. Karavicheva[13], I. Koenig[4], W. Koenig[4], B. W. Kolb[4], G. Kornakov[5], R. Kotte[6], A. Krása[17], F. Krizek[17], R. Krücken[10], H. Kuc[3,16], W. Kühn[11], A. Kugler[17], A. Kurepin[13], V. Ladygin[7], R. Lalik[10,9], J. S. Lange[11], S. Lang[4], K. Lapidus[10,9], A. Lebedev[14], T. Liu[16], L. Lopes[2], M. Lorenz[8], L. Maier[10], A. Mangiarotti[2], J. Markert[8], V. Metag[11], B. Michalska[3], D. Mihaylov[10,9], J. Michel[8], E. Morinière[16], J. Mousa[15], C. Müntz[8], R. Münzer[10,9], L. Naumann[6], Y. C. Pachmayer[8], M. Palka[3], Y. Parpottas[15,f], V. Pechenov[4], O. Pechenova[8], J. Pietraszko[4], W. Przygoda[3], B. Ramstein[16], L. Rehnisch[8], A. Reshetin[13], A. Rustamov[8], A. Sadovsky[13], P. Salabura[3], T. Scheib[8], A. Schmah[a],H. Schuldes[8], E. Schwab[4], J. Siebenson[10], Yu.G. Sobolev[17], S. Spataro[g], B. Spruck[11], H. Ströbele[8], J. Stroth[8,4], C. Sturm[4], A. Tarantola[8], K. Teilab[8], P. Tlusty[17], M. Traxler[4], R. Trebacz[3], H. Tsertos[15], T. Vasiliev[7], V. Wagner[17], M. Weber[10], C. Wendisch[4], J. Wirth[10,9], M. Wisniowski[3], J. Wüstenfeld[6], S. Yurevich[4], Y. Zanevsky[7]

(HADES collaboration)
[1]Istituto Nazionale di Fisica Nucleare - Laboratori Nazionali del Sud, 95125 Catania, Italy
[2]LIP-Laboratório de Instrumentação e Física Experimental de Partículas , 3004-516 Coimbra, Portugal
[3]Smoluchowski Institute of Physics, Jagiellonian University of Cracow, 30-059 Kraków, Poland
[4]GSI Helmholtzzentrum für Schwerionenforschung GmbH, 64291 Darmstadt, Germany
[5]Technische Universität Darmstadt, 64289 Darmstadt, Germany
[6]Institut für Strahlenphysik, Helmholtz-Zentrum Dresden-Rossendorf, 01314 Dresden, Germany
[7]Joint Institute of Nuclear Research, 141980 Dubna, Russia
[8]Institut für Kernphysik, Goethe-Universität, 60438 Frankfurt, Germany
[9]Excellence Cluster 'Origin and Structure of the Universe' , 85748 Garching, Germany
[10]Physik Department E12, Technische Universität München, 85748 Garching, Germany
[11]II.Physikalisches Institut, Justus Liebig Universität Giessen, 35392 Giessen, Germany
[12]Istituto Nazionale di Fisica Nucleare, Sezione di Milano, 20133 Milano, Italy
[13]Institute for Nuclear Research, Russian Academy of Science, 117312 Moscow, Russia
[14]Institute of Theoretical and Experimental Physics, 117218 Moscow, Russia
[15]Department of Physics, University of Cyprus, 1678 Nicosia, Cyprus
[16]Institut de Physique Nucléaire (UMR 8608), CNRS/IN2P3 - Université Paris Sud, F-91406 Orsay Cedex, France
[17]Nuclear Physics Institute, Academy of Sciences of Czech Republic, 25068 Rez, Czech Republic
[18]LabCAF. F. Física, Univ. de Santiago de Compostela, 15706 Santiago de Compostela, Spain

[a] also at Lawrence Berkeley National Laboratory, Berkeley, USA
[b] also at ISEC Coimbra, Coimbra, Portugal
[d] also at Technische Universität Dresden, 01062 Dresden, Germany
[e] also at Dipartimento di Fisica, Università di Milano, 20133 Milano, Italy
[f] also at Frederick University, 1036 Nicosia, Cyprus
[g] also at Dipartimento di Fisica and INFN, Università di Torino, 10125 Torino, Italy

* corresponding author: m.lorenz@gsi.de

Received: 11.04.2016 / Revised version: date

Abstract. The HADES data from p+Nb collisions at a center of mass energy of $\sqrt{s_{NN}}$= 3.2 GeV are analyzed employing a statistical hadronization model. The model can successfully describe the production yields of the identified hadrons π^0, η, Λ, K^0_s, ω with parameters T_{chem} = (99±11) MeV and μ_b = (619±34) MeV, which fits well into the chemical freeze-out systematics found in heavy-ion collisions. In addition, we reanalyze our previous HADES data from Ar+KCl collisions at $\sqrt{s_{NN}}$= 2.6 GeV with an updated version of the model. We address equilibration in heavy-ion collisions by testing two aspects: the description of yields and the regularity of freeze-out parameters from a statistical model fit. Despite this success, the model fails to describe the observed Ξ^- yields in both, p+Nb and Ar+KCl. Special emphasis is put on feed-down contributions from higher-lying resonance states as a possible explanation for the observed excess.

PACS. 25.75.-q, 25.75.Dw

1 Introduction

The idea of applying statistical methods to predict hadron yields in collisions of ions goes back to Heinz Koppe in 1948 [1]. Half a century later statistical hadronization models have been established as a successful tool to describe particle yields or yield ratios from relativistic and ultrarelativistic heavy-ion collisions (HIC) [2–7] with only the parameters T (temperature), μ_B (baryo-chemical potential) and V (volume of the fireball). Moreover, the extracted freeze-out parameters show a striking regularity, lining up on a curve in the temperature - baryochemical potential plane, connecting smoothly data from the lowest energies at SIS18 up to the highest available energy [8,9], describing also the production of light nuclei at LHC [10].
These findings give a strong hint that the observed inclusive, ensemble-averaged hadron abundances are consistent with a state of matter in thermal and chemical equilibrium. However, this does not imply that this state is reached via dynamical equilibration among constituents.
Since the seminal work of Hagedorn [11], statistical methods have also been used to predict particle production in elementary $e^+ + e^-$ and p+p reactions, see e.g. [12]. More recently a detailed analysis applying exactly the same model [4], which successfully describes hadron yields in HIC, shows also a good agreement for yields and even transverse momentum spectra obtained in elementary reactions [13,14]. [1] These findings question conclusions drawn about chemical equilibrium in heavy-ion collisions based on the comparison of data to hadron yields obtained via statistical model calculations and suggest a more fundamental reason for the agreement.
Deviations from equilibrium are included in the models with ad-hoc parameters, whose treatment differs between different realizations. While in [9,16] a grand canonical ensemble with only the parameters T (temperature), μ_B (baryo-chemical potential) and V (volume of the system) is used for central heavy-ion collisions, the authors of [4] use a mixed canonical ensemble, conserving strangeness exactly plus an additional multiplicative factor γ_s in order to additionally suppress particles containing strangeness. In [3], on the other hand, γ_s plus an additional parameter, suppressing the light quarks u,d, called γ_q is used. The authors of [5,17] use also a mixed canonical ensemble, but introduce a strangeness correlation volume parameter V_c (or correlation radius parameter R_c) instead of γ_s. In practice the only effective difference between V_c and γ_s shows up in the predicted yield of the ϕ meson. As the ϕ conserves strangeness by definition, as an $s\bar{s}$ state, its yield is not suppressed in the V_c formalism, while it is strongly suppressed when γ_s is used.
The system size and centrality dependence of those non-equilibrium parameters have been investigated in [18–20]. The authors find a significant increase of the strangeness suppression factor γ_s with increasing system size.
In our previous paper [21] we stated that, by applying a thermal fit to hadron yields obtained from Ar+KCl reactions at 1.76 A GeV, we find that a mixed canonical ensemble with the additional volume parameter V_c (R_c) is necessary to further suppress strangeness to reproduce simultaneously single-strange particle and the ϕ meson yields. While, the double strange Ξ^- hyperon yield overshoots the thermal fit by more than an order of magnitude. Recently, feed down from higher-lying resonances has been proposed as a possible explanation for the observed Ξ^- excess [22].
The hadron spectrum included in the statistical model THERMUS (v2.3) [23], which we used in [21] was based on the 2002 report of the particle data group (PDG) [24] and lacking many high mass resonance states. Those states influence the prediction for low mass particles as well as the fit parameters. It has been updated in THERMUS (v3.0) according to the 2014 report of the particle data group [25] recently. A comparison of the results of the two versions can therefore provide insights on the role of high mass resonances.
In order to understand the origin of the apparent thermal and chemical equilibrium, it is important to consider both the description of yields and regularity of freeze-out parameters by confronting data sets from p+Nb and Ar+KCl using the same statistical model and the same parameters. The detailed statistical analysis of p+A represents the first of its kind in this energy regime where the available yields of different particle species are usually limited. The HADES data allow for the first time a simultaneous fit to eight different measured yields in the same experiment. Special emphasis is put on the effect of the new states in the hadron spectrum, e.g. feed down, included in the PDG report in the last decade.
This paper is organized as follows.
We start with an overview of the two data samples in section 2, before we present and discuss the results of the statistical model fits in 3.1 and 3.2. Section 3.3 is devoted to the Ξ^- excess. Our summary is given in section 4. Finally, in the appendix we include a discussion of statistical strangeness production at high baryochemical potential using exact strangeness conservation.

2 Data sample

HADES is a charged-particle detector consisting of a 6-coil toroidal magnet centered around the beam axis and six identical detection sections located between the coils covering almost the full azimuthal angle. Each sector is equipped with a Ring-Imaging Cherenkov (RICH) detector followed by Multi-wire Drift Chambers (MDCs), two in front of and two behind the magnetic field, as well as a scintillator hodoscope (TOF/TOFino). More abundant hadrons like π^{+-} and p are identified based on their time-of-flight, while for less abundant hadron species like K^{+-} also the energy-loss information from TOF/TOFino, as well as from the MDC tracking chambers are used. The first-level trigger is based on the hit multiplicity in the scintillators covering the same polar angle range between 18° and 85° as the RICH and the tracking detectors. Due to the fixed target setup the rapidity coverage depends

[1] For completeness we refer the reader to another recent statistical analysis reaching different conclusions [15].

on both the particle mass and the kinetic beam energy of the incoming projectile. For the K^0_S it covers roughly 1.5 units in rapidity (around mid-rapidity) at a kinetic beam energy of 1.76 GeV and 1 unit in rapidity (around mid-rapidity) at an energy of 3.5 GeV. Rapidity distributions of the different identified hadrons are obtained by integrating transverse mass spectra for each bin in rapidity, using Boltzmann distributions fitted to the data points, for extrapolation to the regions not covered by active detectors. The obtained rapidity distributions are fitted with Gaussian like distributions, which are used to obtain the hadron yields in full phase space. Details may slightly vary for the various hadrons and are discussed in the corresponding references given below. The extracted inverse slope T_{eff} of the transverse mass spectra at mid-rapidity includes a pure kinetical component T_{kin} plus an additive term, depending on the particle mass m and the square of the radial expansion velocity of the system β. Note that in case of p+A collisions no radial expansion of the fireball is expected. However, additional effects like resonance decays deform the spectra, as demonstrated in [26–28] in case of ϕ feed-down to K^- spectra. For further information on radial expansion of the fireball and the relation to the kinetic freeze-out temperature, we refer the reader to [29–31]. A detailed description of the HADES detector is given in [32].

2.1 Ar+KCl at $\sqrt{s_{NN}}$= 2.6 GeV

An argon beam of $\sim 10^6$ particles/s was incident with a beam energy of 1.76A GeV on a four-fold segmented KCl target with a total thickness corresponding to 3.3 % interaction probability. A fast diamond start detector located upstream of the target intercepted the beam and was used to determine the time-zero information. The data readout was started by a first-level trigger (LVL1) requiring a charged-particle multiplicity, $MUL \geq 16$, in the scintillator hodoscope. Note that only protons, which are the most abundant charged particles at this energy, with momenta larger than 300 MeV/c in the laboratory reference frame can hit the scintillator array due to their bending in the magnetic field of HADES. Based on a full GEANT simulation of the detector response to Ar+KCl events generated with the UrQMD transport model [40], we found that the event ensemble selected by this (LVL1) trigger condition has a mean number of participating nucleons $\langle A_{part} \rangle$ of 38.5 ± 4 corresponding to about 35% most central collisions [21]. In total 7.4×10^8 LVL1 events have been collected. The yields of the various identified particles obtained in [21,33–39] and their inverse slope parameter T_{eff} obtained from fitting Boltzmann distributions to the transverse mass spectra at mid-rapidity are listed in Tab. 1.
The bias of the second level trigger (LVL2) used to trigger on electrons and relevant for the ω yield is about of 10% and is corrected for.
We decided to include the yield of the η meson which is not measured by HADES but rather interpolated from TAPS measurements in Ar(Ca)+Ca collisions at 1.5 and 2 A GeV [41,42]. Note that in previous works the η meson yield was not well described by a statistical model approach [5]. The measured energy excitation function of the η meson yield is parametrized and interpolated using a polynomial fit [42]. The difference in centrality selections of the two experiments is accounted for by assuming a linear dependence of the η yield with $\langle A_{part} \rangle$. Further details on the used excitation functions are given in [42].

2.2 p+Nb at $\sqrt{s_{NN}}$= 3.2 GeV

A proton beam of about 2×10^6 particles/s with kinetic energy of 3.5 GeV was incident on a 12-fold segmented target of niobium (^{93}Nb). The first-level (LVL1) trigger required a charged-particle multiplicity $MUL \geq 3$ in the scintillator hodoscope. The selected event sample corresponds to the 90% most central collisions. This estimation is obtained using two different Monte-Carlo models [40, 44] in combination with a small fraction of the data taken with a trigger condition requiring only a charged-particle multiplicity of $MUL \geq 2$ in the scintillator hodoscope. About 3.2×10^9 LVL1 events have been collected. The yields of the various identified particles obtained in [45–48] and their inverse slope parameter T_{eff} derived from fitting Boltzmann distributions to the transverse mass spectra are listed in Tab. 2. The value for $\langle A_{part} \rangle$ is obtained from a geometrical overlap model [49,50], where we used a very conservative error estimation of 20% in total. The full phase space yield of the ω meson is based on a GiBUU transport code which describes the data very satisfactorily within the HADES acceptance [49,51,52].

3 Statistical model fit to hadron yields

3.1 Ar+KCl at $\sqrt{s_{NN}}$= 2.6 GeV

We apply a similar fit as in our previous work [21] but use the updated version (v3.0) of THERMUS [23]. The main difference to the previously used version (v2.3) is the included hadron spectrum which was updated from the PDG report 2002 [24] to the one from 2014 [25], including now several new strange states, e.g. K*(800), as well as states containing charm, which are not relevant here. In addition, we include now in the fit the experimental yields of the p, ω and $K^*(892)^0$ which have become available recently [33,37,38].
We use the mixed canonical ensemble where strangeness is exactly conserved while all other quantum numbers are calculated grand canonically and fix the charge chemical potential μ_Q using the ratio of the baryon and charge numbers of the collision system.
The yield of the ϕ meson is of particular interest, because of its sensitivity to the strangeness suppression parameters γ_s and R_c. Being an $s\bar{s}$ state the ϕ conserves strangeness by definition. Its yield is not suppressed in the R_c formalism, while strongly suppressed when γ_s is used. We found in [21] that the yield is well described using R_c and

Table 1. Multiplicities (i.e. yield in full phase space per LVL1 event) and effective temperatures T_{eff} of particles produced in Ar(1.76 A GeV)+KCl reactions. If only a single error is given, the value corresponds to the total error, including systematic and statistical uncertainties. A "–" in the T_{eff} column means that the statistics in the spectra is not sufficient to extract a T_{eff} value. The acronyms (syst) and (extr) stand for systematical and extrapolation respectively and are used to indicate the systematic uncertainties within the HADES acceptance and the one due to extrapolation in rapidity to full phase space.

Particle	Multiplicity	T_{eff} [MeV]	Reference
$\langle A_{part} \rangle$	38.5 ± 4	–	[21,40]
p	22.11 ± 2.4	142 ± 5	[33]
π^-	$3.9 \pm 0.19 \pm 0.34$(syst)	$82.4 \pm 0.1^{+9.1}_{-4.6}$	[34]
η	0.081 ± 0.02	–	[41,42]
$\Lambda + \Sigma^0$	$(4.09 \pm 0.1 \pm 0.17$ (extr)$^{+0.17}_{-0.37}$ (syst)$) \times 10^{-2}$	$95.5 \pm 0.7 + 2.2$	[21]
K^+	$(2.8 \pm 0.2 \pm 0.1$(syst)± 0.1(extr)$) \times 10^{-2}$	$89 \pm 1 \pm 2$	[35]
K^0_S	$(1.15 \pm 0.05 \pm 0.09$(syst)$) \times 10^{-2}$	92 ± 2	[36]
K^-	$(7.1 \pm 1.5 \pm 0.3$(syst)± 0.1(extr)$) \times 10^{-4}$	$69 \pm 2 \pm 4$	[35]
$K^*(892)^0$	$(4.4 \pm 1.1 \pm 0.5$(syst)$) \times 10^{-4}$	–	[37]
ω	$(6.7 \pm 2.7) \times 10^{-3}$	131 ± 26	[38]
ϕ	$(2.6 \pm 0.7 \pm 0.1 - 0.3) \times 10^{-4}$	84 ± 8	[35]
Ξ^-	$(2.3 \pm 0.9) \times 10^{-4}$	–	[39]

Table 2. As in Tab. 1 but for p(3.5GeV)+Nb reactions.

Particle	Multiplicity	T_{eff} [MeV]	Reference
$\langle A_{part} \rangle$	2.8 ± 0.6	–	[49,50]
π^0	$0.66 \pm 0.06 \pm 0.1$(syst)	92 ± 3 combined fit with π^-	[45]
π^-	0.6 ± 0.1	92 ± 3 combined fit with π^0	[45]
η	$0.034 \pm 0.002 \pm 0.008$(syst)	84 ± 3	[45]
$\Lambda + \Sigma^0$	0.017 ± 0.003	92 ± 5	[46]
K^0_S	0.0055 ± 0.0007	99 ± 4	[47]
ω	0.007 ± 0.004	–	[49,51,52]
Ξ^-	$(2.0 \pm 0.4 \pm 0.6$(syst)$) \times 10^{-4}$	–	[48]

therefore stick to this way of suppressing strange particle yields in our statistical model calculations. Note that at higher energies and small systems the description of the ϕ meson yield improves when additional suppression parameters are introduced [17].

We fit simultaneously all particle yields listed in Tab. 1, as well as the mean number of participants $\langle A_{part} \rangle$ (defined as the number of net-baryons within THERMUS and hence applicable mainly at low energies). We find the following values for chemical freeze-out parameters $T_{chem} = (70 \pm 3)$ MeV, $\mu_b = (748 \pm 8)$ MeV, the strangeness correlation radius results as $R_c = (2.9 \pm 0.1)$ fm and the radius of the whole fireball $R = (5.7 \pm 0.8)$ fm with a χ^2/d.o.f. [2] of 3.6. A detailed comparison of the data with the statistical model fit is shown in the upper part of Fig. 1, while the lower part depicts the ratio of data to the THERMUS value. As reported previously [21], the Ξ^- yield is not reproduced by the model and hence a number is displayed instead of a data point.

Comparing the particle yields, the strongest deviations are observed for the protons, the η and the Ξ^-. Already the results presented in [43] pointed out that the yield of the η meson seems to favor a significantly higher freeze-out temperature. However, we want to point out that about half of its yield results from decays of baryon-resonances mainly $N(1535)$ in THERMUS. Hence, also the precise knowledge of the resonance spectrum and the corresponding branching ratios to final states are of great importance for the description of the η meson yield.

In the sector of the vector mesons, both the yields of the ω and the ϕ are in favor of a slightly higher temperature, while the $K^*(892)^0$ yield is better described with a lower temperature. The latter observation is made also at higher energies and has been interpreted in the following way: due to the short life time of the $K^*(892)^0$, its decay products could be rescattered inside the medium [53], making the resonance not reconstructable. At the same time the decay products of the ϕ meson are less affected, as the ϕ decays mainly outside of the medium due to its longer lifetime. The comparison of resonances with different lifetimes could provide an estimate of the lifetime of the hadronic phase.

These values for the obtained freeze-out parameters may be compared to the values of $T_{chem} = (76 \pm 2)$ MeV, $\mu_b = (799 \pm 22)$ MeV, $R_c = (2.2 \pm 0.2)$ fm, $R = (4.1 \pm 0.5)$ fm and χ^2/d.o.f. of 2.6 obtained for the same system in [21]. We observe a deviation of all parameters at the order of a few standard deviations. While the percentaged deviation is only at the order of 5% for T and μ_b it is about 25%

[2] Defined as the number of particle yields included in the fit minus the number of free parameters.

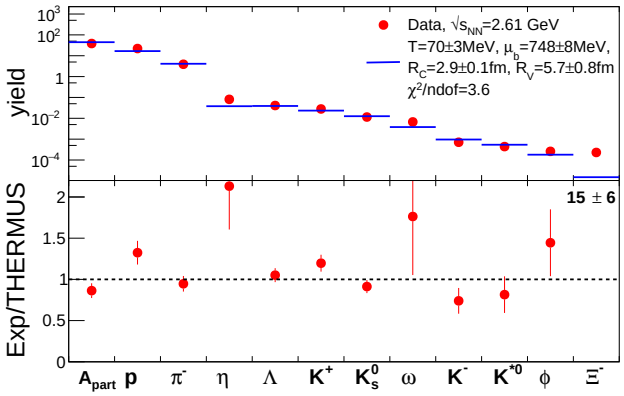

Fig. 1. Yields (filled red circles) of hadrons in Ar+KCl reactions and the corresponding THERMUS fit values (blue bars). The lower plot shows the ratio of the experimental value and the THERMUS value. For the Ξ^- the value of the ratio is quoted instead of displaying a point.

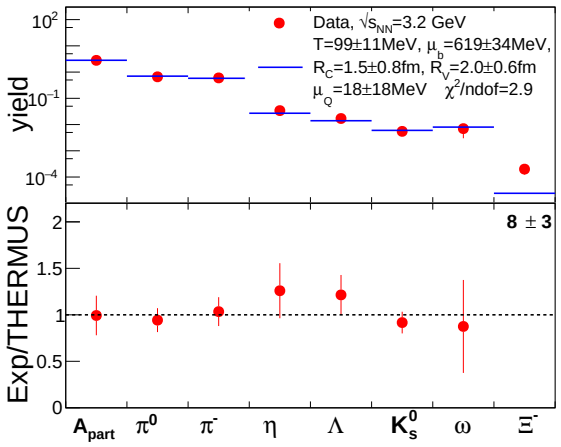

Fig. 2. Yields of hadrons in p+Nb reactions (filled red circles) and the corresponding THERMUS fit (blue bars). The lower plot shows the ratio of the experimental value and the THERMUS value. For the Ξ^- the value of the ratio is quoted instead of displaying a point.

for the radii. Due to correlations between all four parameters the minimum of the fit moves to a slightly different position in the parameter space as a result of an interplay of several effects. As more hadron states are included, the baryochemical potential is slightly lower, which is to some extent compensated by a larger volume. Due to this larger volume the temperature T is slightly lower as otherwise the pion rate would overshoot the experimental values.
Also the χ^2/d.o.f. of 3.6 (3.3 when not including the Ξ^- yield like in the previous work) is worse compared to the previous fit [21] results. The observed deviation in the parameter values compared to our previous work, are indicative of the systematic model uncertainty.
The excess of the experimentally measured Ξ^- yield over the model decreases from a factor 24 ± 9 to a factor 15 ± 6 when using the actual version (v3.0) of THERMUS. We will come back to this in the discussion of the Ξ^- excess.
In order to disentangle the effects due to the different set of particles included in the fit and of the newly included hadron states we refit the same Ar+KCl yields ($\langle A_{part} \rangle$, π^-, Λ, K^0_s, K^+, K^-, ϕ) like in our previous work [21]. We find $T_{chem} = (72 \pm 3)$ MeV, $\mu_b = (757 \pm 14)$ MeV, $R_c = (2.7 \pm 0.2)$ fm, $R = (5.0 \pm 1)$ fm which agree within the stated errors with the parameter values obtained for the full particle sample. The differences in the obtained parameter minimum, can therefore be indeed attributed to the different hadron spectrum used as input to the model.
The comparison of the extracted chemical freeze-out temperature T_{chem} to the ones extracted from the inverse slope T_{eff} of transverse mass spectra at mid-rapidity for various particles listed in Tab. 1 is not straightforward. As discussed, the extracted inverse slope parameter T_{eff} includes a pure kinetical component T_{kin} plus an additive term, depending on the particle mass m and the square of the radial expansion velocity β as well as additional effects like resonance decays.

3.2 p+Nb at $\sqrt{s_{NN}}$= 3.2 GeV

For the fit to the yields obtained from p+Nb reactions we add the charge chemical potential μ_Q as an additional free parameter due to the strong asymmetry of the collision system. Apart from the charge chemical potential μ_Q, we use the same parameters as above. The extracted parameters are $T_{chem} = (99 \pm 11)$ MeV, $\mu_b = (619 \pm 34)$ MeV, $\mu_Q = (18 \pm 18)$ MeV, $R_c = (1.5 \pm 0.8)$ fm, $R = (2.0 \pm 0.6)$ fm and χ^2/d.o.f. of 2.9. As μ_Q agrees within the given errors with 0, we also apply a fit with a fixed $\mu_Q = 0$ and find that all other parameters change only slightly, well covered by the stated errors. A detailed comparison of the data with the statistical model fit is shown in the upper part of Fig. 2, while the lower part of this figure depicts the ratio of data to the THERMUS values. Again, in case of the Ξ^-, a number is displayed instead of a point.
Within errors, the values for R and R_c agree with each other, as the suppression of strangeness is dominated by the overall small volume.
The ratio between data and model show striking similarities when comparing the Ar+KCl values in Fig. 1 with the ones of p+Nb in Fig. 2. In both cases the model is able to describe with fair agreement most of the yields but fails by nearly an order of magnitude in case of the Ξ^-.
Similar to the Ar+KCl fit the excess of the experimentally measured Ξ^- yield over the model decreases from a factor 20 ± 9 as reported in [48] to a factor 8 ± 3 when using the current THERMUS version (v3.0).
The comparison of the extracted chemical freeze-out temperature T_{chem} to the ones extracted from the inverse slopes of transverse mass spectra at mid-rapidity for various particles listed in Tab. 2 is more straightforward than in case of Ar+KCl, as we expect no strong collective expansion of the system [29]. Indeed, the extracted slopes

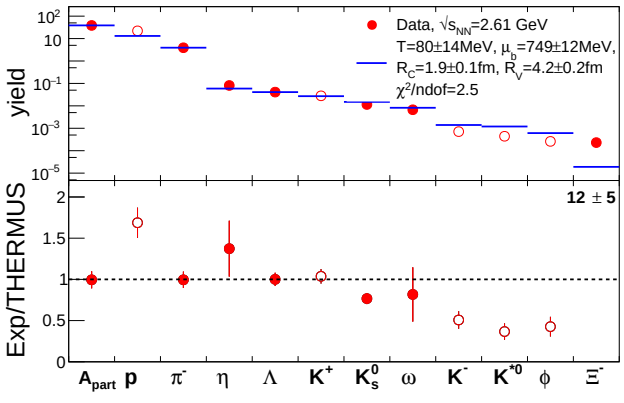

Fig. 3. As in Fig. 1 but excluding the p, K^+, K^-, $K^*(892)^0$, ϕ yields, shown by open symbols, in the fit.

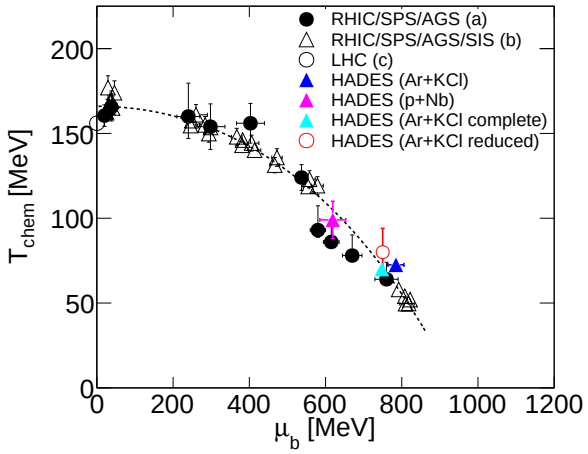

Fig. 4. Chemical freeze-out points in the T_chem – μ_b plane. The filled black circles (a) are taken from [16], the black open triangles (b) are from [8] and the black open circle (c) from [9]. The presented fit results are defined in the legend. The dashed curve correponds to a fixed energy per nucleon of 1 GeV, calculated according to [8]. The dark blue triangle corresponds to our Ar+KCl fit presented in [21], the light blue triangle shows the result obtained for the full sample and open circle to the reduced data sample both presented in this work.

show no significant dependence on the particle mass with an average value of $\langle T_{kin} \rangle = (91 \pm 2)$ MeV, which is in agreement with the value for the chemical freeze-out temperature extracted from the statistical fit of $T_{chem} = (99 \pm 11)$ MeV.

In order to further discuss the similarities between the Ar+KCl and the p+Nb fit, we reduce our larger Ar+KCl data sample to the same set of identified hadron species as in the p+Nb sample, by excluding the yields of the p, K^+, K^-, $K^*(892)^0$ and the ϕ in our fit. [3] For the reduced Ar+KCl fit we find $T_{chem} = (80 \pm 14)$ MeV, $\mu_b = (749 \pm 12)$ MeV, $R_c = (1.9 \pm 0.1)$ fm, $R = (4.2 \pm 0.2)$ fm and χ^2/d.o.f. of 2.5. The comparison between data and model is shown in a similar way as above in Fig. 3.

By restricting the Ar+KCl sample to a comparable one as available for p+Nb we find a variation of the freeze-out parameters of order 5%, consistent with the systematic uncertainty of such an analysis.

The χ^2/d.o.f. of the Ar+KCl fits of 3.6 and 2.5 are comparable to the one obtained for the p+Nb sample of 2.9. Also the absolute average differences of model to data ratio is smaller in the p+Nb case (13%) compared to (32%) for the Ar+KCl fit. This is rather surprising as one naively expects that the larger Ar+KCl system is closer to chemical and thermal equilibrium and hence less deviation from statistical equilibrium values. Note that the average number of participants is smaller than 3 in case of the p+Nb sample. Furthermore, the p+Nb freeze-out point fits at least as well as the Ar+KCl points to the previously observed regularity of freeze-out points in the $T_{chem} - \mu_b$ plane, displayed in Fig. 4, where the extracted points of this work are displayed together with similar points extracted in [8,9,16].

This brings us back to the motivation of our analysis stressed in the introduction: While the success of the statistical model in describing particle rates from heavy-ion collisions is often implicitly connected to a thermalization of the created system, the success of the model for the p+Nb data at $\sqrt{s_{NN}} = 3.2$ GeV questions this connection. In this context we refer the reader to a very recent publication [58], where the authors investigate further the origin of this apparent equilibrium by comparing rates from a transport model at different time steps of a heavy-ion collision to those obtained from a statistical hadronization model.

Apart from such conceptual issues we stress that T_{chem} for p+Nb at $\sqrt{s_{NN}} = 3.2$ GeV is "naturally" somewhat larger than T_{chem} for Ar+KCl at $\sqrt{s_{NN}} = 2.6$ GeV which one could attribute to the higher energies in primary collisions producing secondary hadrons. Analogously, μ_b in Ar+KCl is larger than for p+Nb, since some noticeable compression is expected in heavy-ion collisions. In addition, the authors of [54] find also a slight dependence on the system size of T_{chem}.

3.3 On the Ξ^- puzzle

Several mechanisms have already been proposed to explain the excess of the Ξ^- yield in Ar+KCl. However, the presence of the excess of the Ξ^- in p+A collisions has several interesting implications for the interpretation of the heavy-ion data as its origin seems to be already in the elementary channels without the involvement of many-body effects in the medium. Therefore, the increased cross sections of strangeness exchange reactions, which were found to be sufficient to explain the high yield in [55,56], seem to be questionable as they are unlikely to play an important role in p+Nb reactions. Also the invoked [57] catalytic

[3] As the yield of the neutral pions is not directly available, we restrict μ_Q by the initial neutron to proton ratio.

strangeness production by secondary processes, such as $\pi + Y \rightarrow \Xi + K$, are strongly suppressed in p+A collisions.

Production via the high mass tails of intermediate resonances has been proposed recently in [22] as another possible explanation. The authors tuned the mass dependent branching ratio of high-lying baryon resonances, namely the $N^*(1990)$, $N^*(2080)$, $N^*(2190)$, $N^*(2220)$ and $N^*(2250)$, in a transport code to match elementary data on ϕ meson production. As a result the ϕ/K^- ratio in Ar+KCl is successfully reproduced. The same mechanism is then also used for the Ξ^- hyperon but due to the lack of elementary data, the model is tuned to match our p+Nb data.

The technique of mass dependent branching ratios for broad resonances has been successfully applied in order to describe the dilepton spectra at low energies as pointed out in [51,59]. Although the tuned branching ratios are still consistent with the OZI rule, there is no established experimental evidence for the decay of the N^* resonances to final states containing a ϕ meson or a Ξ hyperon. Therefore, there is no branching of N^* resonances to double-strange final states included in THERMUS.

In addition, the total yield of the five above discussed N^* resonances amounts to 1.47×10^{-3} and 7.1×10^{-4} in THERMUS for the Ar+KCl and the p+Nb data sample respectively. In order to explain the observed Ξ^- yields which are of order 10^{-4} in both systems, branching ratios of the N^* resonances to Ξ^- of order 10% or higher would be needed. This is a very similar value as the one quoted by the authors of [22]. Such a large branching ratio and corresponding contributions from high-lying N^* resonances should manifest itself in a dedicated p+p experiment slightly above Ξ^- the elementary production threshold, either directly in the angular distribution of produced Ξ^- (similar to our analysis presented in [60]) or with the help of a more sophisticated partial wave analysis searching explicitly for an upper limit on the branching ratio N^* to final Ξ^- states (similar like our analysis searching for kaonic clusters in [61]). We are currently working out the best experimental setup for a future HADES experiment addressing these issue.

The feed down to Ξ hyperons in THERMUS is mainly originating from the decay of excited Ξ(1530, 1690, 1820, 1950, 2030) and some higher-lying Λ and Σ states. Note that the widths, branching ratios etc. of these states are not well constrained and subject of current and future scientific activities [62,63]. The feed down fraction to the Ξ^- yield amounts to 10% and 27% percent of the total rate in THERMUS, respectively, for Ar+KCl and p+Nb. From these numbers it becomes clear that the difference in yields of the double-strange hyperons between the two used THERMUS versions is not due to additional higher-lying states and corresponding feed-down. In addition, it is very unlikely that unknown strange states in the hadron spectrum could contribute more than an order of magnitude more yield than the known ones and hence explain the excess of the Ξ^- yield. The difference between the two THERMUS version in the Ξ^- yield is however connected to the new states in the hadron spectrum via the mechanism for exact strangeness conservation using the strangeness correlation volume V_c (see appendix A for more details). As there are more hadronic (mesonic) states included in the current version, the probability for counterbalancing the strange quarks of the hyperons is higher for a given volume. Especially the rather low-lying scalar meson $K^*(800)^{0+}$ (also known as κ) is important in this context as its abundance is still not too rare. However, one should note that, with a widths of $\Gamma \approx 500$ MeV, evidences for this state are hard to establish. The effect on the yield is much more prominently seen in the double-strange baryon sector because their yield scales with the volume proportional to the power of three, see Eq. (6), compared to the one of single-strange particles whose yield scales only quadratically with the volume, see Eq. (5).

From this consideration it becomes clear that a precise knowledge of the hadron spectrum is an important ("counterbalancing the strange quarks of the hyperons") issue for the interpretation of HIC data.

4 Summary and Outlook

By comparing the obtained freeze-out parameters from a statistical model fit to HADES data obtained from p+Nb and Ar+KCl collisions at center of mass energies of $\sqrt{s_{NN}}$ = 3.2 GeV and $\sqrt{s_{NN}}$ = 2.6 GeV respectively, we tried to address the aspect of equilibration in HIC by testing two manifestations, the description of yields and regularity of freeze-out parameters. We make the rather surprising finding that the statistical model is able to describe the p+Nb data as well as the larger system the Ar+KCl data, which questions the often drawn connection between the agreement of statistical models with particle yields in heavy-ion collisions and thermalization.

Furthermore, we emphasize that the excess of the Ξ^- is already present in cold nuclear matter. Given the rates of higher-lying N^* resonances predicted by our statistical model fit, we find feed down of these states only a plausible explanation if their branching ratio to Ξ^- final states is at the order of 10% or higher. Such a large branching ratio should manifest itself in experimental observables in a dedicated p+p experiment with HADES, slightly above the elementary Ξ^- threshold. In addition, we want to point out that HADES data of central Au+Au collisions will be come available soon and might allow to gather further insights into the subject.

Acknowledgments

LIP Coimbra, Coimbra (Portugal) PTDC/FIS/113339/ 2009 SIP JUC Cracow, Cracow (Poland) NCN grant 2013/ 10/M/ ST2/00042, N N202 286038 28-JAN-2010 NN202198639 01-OCT-2010 Helmholtz-Zentrum Dresden-Rossendorf (HZDR), Dresden (Germany) BMBF 06DR9059D

TU München, Garching (Germany) MLL München DFG EClust 153 VH-NG-330 BMBF 06MT9156 TP5 GSI TMKrue 1012 NPI AS CR, Rez, Rez (Czech Republic) MSMT LC07050 GAASCR IAA100480803 USC - S. de Compostela, Santiago de Compostela (Spain) CPAN: CSD2007-00042 Goethe-University, Frankfurt (Germany)

HA216/EMMI HIC for FAIR (LOEWE) BMBF: 06FY9100I GSI FE EU Contract No. HP3-283286. One of us (M.L.) acknowledges the support of the Humboldt Foundation.

References

1. H. Koppe, Z. Naturforschg. 3 a, 251 (1948).
2. P. Braun-Munzinger, K. Redlich and J. Stachel, arXiv:nucl-th/0304013 (2003).
3. M. Petran, J. Letessier, V. Petracek and J. Rafelski, Phys. Rev. C **88**, 034907 (2013).
4. F. Becattini, M. Gazdzicki, A. Keranen, J. Manninen and R. Stock, Phys. Rev. C **69**, 024905 (2004).
5. J. Cleymans, H. Oeschler and K. Redlich, Phys. Rev. C **59**, 1663 (1999).
6. A. N. Tawfik, Int. J. Mod. Phys. A **29**, 1430021 (2014).
7. M. Floris, Nucl. Phys. A **931**, 103 (2014).
8. J. Cleymans, H. Oeschler, K. Redlich and S. Wheaton, Phys. Rev. C **73**, 034905 (2006).
9. J. Stachel, A. Andronic, P. Braun-Munzinger and K. Redlich, J. Phys. Conf. Ser. **509**, 012019 (2014).
10. J. Adam *et al.* [ALICE Collaboration], Phys. Rev. C **93** no.2, 024917 (2016).
11. R. Hagedorn, Nuovo Cim. Suppl. **3**, 147 (1965).
12. E. V. Shuryak, Yad. Fiz. **16**, 395 (1972).
13. F. Becattini and G. Passaleva, Eur. Phys. J. C **23**, 551 (2002).
14. F. Becattini, P. Castorina, J. Manninen and H. Satz, Eur. Phys. J. C **56**, 493 (2008).
15. A. Andronic, F. Beutler, P. Braun-Munzinger, K. Redlich and J. Stachel, Phys. Lett. B **675**, 312 (2009).
16. A. Andronic, P. Braun-Munzinger and J. Stachel, Nucl. Phys. A **772**, 167 (2006).
17. I. Kraus, J. Cleymans, H. Oeschler, K. Redlich and S. Wheaton, Phys. Rev. C **76**, 064903 (2007).
18. J. Cleymans, B. Kämpfer, P. Steinberg and S. Wheaton, J. Phys. G **30**, S595 (2004).
19. B. Kämpfer, J. Cleymans, P. Steinberg and S. Wheaton, Heavy Ion Phys. **21**, 207 (2004).
20. J. Cleymans, B. Kampfer, M. Kaneta, S. Wheaton and N. Xu, Phys. Rev. C **71**, 054901 (2005).
21. G. Agakishiev *et al.* [HADES Collaboration], Eur. Phys. J. A **47**, 21 (2011).
22. J. Steinheimer and M. Bleicher, J. Phys. G **43** 1, 015104 (2016).
23. S. Wheaton and J. Cleymans, Comput. Phys. Commun. **180**, 84 (2009).
24. K. Hagiwara et al. (Particle Data Group), Phys. Rev. D **66**, 010001 (2002).
25. K. A. Olive *et al.* [Particle Data Group Collaboration], Chin. Phys. C **38**, 090001 (2014).
26. M. Lorenz *et al.* (HADES Collaboration), PoS (BORMIO2010) 038 (2010).
27. K. Piasecki *et al.* [FOPI Collaboration], Phys. Rev. C **91**, 054904 (2015).
28. P. Gasik *et al.* [FOPI Collaboration], arXiv:1512.06988 [nucl-ex].
29. N. Herrmann, J. P. Wessels and T. Wienold, Ann. Rev. Nucl. Part. Sci. **49** 581 (1999).
30. W. Reisdorf and H. G. Ritter, Ann. Rev. Nucl. Part. Sci. **47** 663 (1997). d
31. W. Reisdorf *et al.* [FOPI Collaboration], Nucl. Phys. A **848** 366 (2010).
32. G. Agakishiev *et al.* [HADES Collaboration], Eur. Phys. J. A **41**, 243 (2009).
33. H. Schuldes *et al.* [HADES Collaboration], J. Phys. Conf. Ser. **599**, 012028 (2015).
34. P. Tlusty *et al.* [HADES Collaboration], arXiv:0906.2309 (2009).
35. G. Agakishiev *et al.* [HADES Collaboration], Phys. Rev. C **80**, 025209 (2009).
36. G. Agakishiev *et al.* [HADES Collaboration], Phys. Rev. C **82**, 044907 (2010).
37. G. Agakishiev *et al.* [HADES Collaboration], Eur. Phys. J. A **49**, 34 (2013).
38. G. Agakishiev *et al.* [HADES Collaboration], Phys. Rev. C **84**, 014902 (2011).
39. G. Agakishiev *et al.* [HADES Collaboration], Phys. Rev. Lett. **103**, 132301 (2009).
40. S. A. Bass *et al.*, Prog. Part. Nucl. Phys. **41**, 225 (1998).
41. F. D. Berg *et al.*, Phys. Rev. Lett. **72** 977 (1994).
42. R. Holzmann *et al.* [TAPS Collaboration], Phys. Rev. C **56** 2920 (1997).
43. R. Averbeck, R. Holzmann, V. Metag and R. S. Simon, Phys. Rev. C **67**, 024903 (2003).
44. O. Buss *et al.*, Phys. Rept. **512** (2012).
45. G. Agakishiev *et al.* [HADES Collaboration], Phys. Rev. C **88**, 024904 (2013).
46. G. Agakishiev *et al.* [HADES Collaboration], Eur. Phys. J. A **50**, 81 (2014).
47. G. Agakishiev *et al.* [HADES Collaboration], Phys. Rev. C **90**, 054906 (2014).
48. G. Agakishiev *et al.* [HADES Collaboration]. Phys. Rev. Lett. **114**, 212301 (2015).
49. G. Agakishiev *et al.* [HADES Collaboration], Phys. Lett. B **715**, 304 (2012).
50. R. J. Glauber and G. Matthiae, Nucl. Phys. **B 21**, 135 (1970).
51. J. Weil, H. van Hees and U. Mosel, Eur. Phys. J. A **48**, 111 (2012).
52. J. Weil, private communication of the corresponding omega yield in full phase space.
53. C. Markert, G. Torrieri and J. Rafelski, AIP Conf. Proc. **631**, 533 (2002).
54. F. Becattini, J. Manninen and M. Gazdzicki, Phys. Rev. C **73**, 044905 (2006).
55. F. Li, L. W. Chen, C. M. Ko and S. H. Lee, Phys. Rev. C **85**, 064902 (2012).
56. G. Graef, J. Steinheimer, F. Li and M. Bleicher, Phys. Rev. C **90**, 064909 (2014).
57. E. E. Kolomeitsev, B. Tomasik and D. N. Voskresensky, Phys. Rev. C **86**, 054909 (2012) .
58. J. Steinheimer, M. Lorenz, F. Becattini, R. Stock and M. Bleicher, arXiv:1603.02051 [nucl-th].
59. E. L. Bratkovskaya, J. Aichelin, M. Thomere, S. Vogel and M. Bleicher, Phys. Rev. C **87**, 064907 (2013).
60. G. Agakishiev *et al.* [HADES Collaboration], Phys. Lett. B **742** 242 (2015).
61. G. Agakishiev *et al.* [HADES Collaboration], Phys. Rev. C **85** 035203 (2012).
62. M. Ronniger and B. Ch. Metsch, Eur. Phys. J. A **47**, 162 (2011).
63. M.F.M. Lutz *et al.* [PANDA Collaboration], arXiv:0903.3905 (2009).

A Statistical strangeness production at high baryo-chemical potential using exact strangeness conservation

In a pure statistical ansatz based on the common temperature T of all species and the baryo-chemical potential μ_B, the multiplicities of mesons and baryons produced in a heavy-ion collision, neglecting feed-down and isospin asymmetry are given by

$$\sum_i M_{m_i} = \sum_i g_i V \int \frac{d^3p}{(2\pi)^3} \exp\left(-\frac{E_i}{T}\right) \times F_{Si}, \quad (1)$$

$$\sum_j M_{b_j} = \sum_j g_j V \int \frac{d^3p}{(2\pi)^3} \exp\left(-\frac{E_j - \mu_B}{T}\right) \times F_{Sj}, \quad (2)$$

with M_{m_i} and M_{b_j} being the multiplicities of a given meson (m) or baryon (b), the degeneracy factors $g_{i,j}$, the volume of the fireball V and the energies of the corresponding meson and baryon $E_{i,j} = \sqrt{m_{i,j}^2 + p_{i,j}^2}$.
Particles containing strangeness are rare, especially at SIS energies, and therefore the strange quantum number must be exactly conserved in each event in the ensemble; each particle carrying a strange quark must be counterbalanced by one carrying an antistrange quark due to associated strangeness production in strong-interaction processes. This results in a multiplicative canonical suppression factor $F_S(T, \mu_B, V, S, N_S)$, which is equal to one for non-strange particles and approaches, in the limit of large volumes and temperatures, the grand canonical fugacities $\lim_{V,T\to\infty} F_{Si,j} = exp\,(-S_{i,j}\mu_S/T)$. The factor $F_{Si,j}$ for each particle species i, j depends in general on the thermodynamical properties of the system, the strangeness content $S_{i,j}$ of the respective particle and the number of meson and baryon states containing strangeness N_S.
We illustrate the effect of F_S by making use of the opposite limit of small volume and temperature, where particle numbers are small and the canonical strangeness suppression is most relevant. For $M < 1$ the multiplicity of kaons M_{m_K} can be approximated as

$$M_{m_K} \approx g_K V \int \frac{d^3p}{(2\pi)^3} \exp\left(-\frac{E_K}{T}\right) \times \left[g_Y V \int \frac{d^3p}{(2\pi)^3} \exp\left(-\frac{E_Y - \mu_B}{T}\right) + g_{\overline{K}} V \int \frac{d^3p}{(2\pi)^3} \exp\left(-\frac{E_{\overline{K}}}{T}\right) \right]. \quad (3)$$

The two terms inside the square brackets correspond to the counterbalance terms for the antistrange quark inside the kaons from the hyperons and from the antikaons. Hence Eq. (3) can be rewritten as

$$M_{m_K} \approx M_{m_K}^{GC} \times \left[M_{m_Y}^{GC} + M_{m_{\overline{K}}}^{GC} \right] \quad (4)$$

with $M_{b_Y}^{GC}, M_{m_K}^{GC}$ and $M_{m_{\overline{K}}}^{GC}$ corresponding to the grand-canonical multiplicities of kaons, hyperons and antikaons, respectively. As we assume T and V to be sufficiently small, so that $M < 1$, one can clearly see the resulting suppression due to exact strangeness conservation. Due to the absence of antimatter at high μ_B the counterbalance term for the antikaons by the antihyperons is missing, resulting in a stronger suppression compared to kaons. Hence for $(E_Y - \mu_B) \ll E_K$ we can neglect the antikaon term and approximate the multiplicity of single-strange hyperons as

$$M_{b_Y} \approx M_{b_Y}^{GC} \times \left[M_{m_K}^{GC} \right] \propto V^2. \quad (5)$$

Compared to non-strange particle multiplicities, which are proportional to V the multiplicity of single-strange particles is proportional to V^2 for small systems. Rewriting Eq. (5) for double-strange hyperons, like the Ξ, one finds their yield scaling with V^3:

$$M_{b_\Xi} \approx M_{b_\Xi}^{GC} \times \left[M_{m_K}^{GC} \right]^2 \propto V^3. \quad (6)$$

The above mentioned strangeness correlation volume V_c, in which strangeness has to be exactly conserved, is realized by setting the volume terms in the brackets in Eq. (3) to V_c. For $V_c < V$, strange particles are suppressed additionally on top of the pure canonical suppression.
From these considerations it becomes clear that the size of F_S for a given volume V_c and hence the strength of the suppression depends also on the number of known strange particle states. The more states exist the more possibilities are available for counterbalancing the strange (antistrange) quarks. This is of relevance for the comparison of the different THERMUS versions 2.3 and 3.0. The latter one has more states included, especially the rather low lying K*(800) states are important in this context.